Proceedings of ICRC 2001: 1799 © Copernicus Gesellschaft 2001

ICRC 2001

Plerion as a source of primary cosmic ray electrons

S. A. Stephens

Laboratory for High Energy Physics, Code 661, NASA/GSFC, Greenbelt, MD 20771, U.S.A.

Abstract.

Positrons (e^+) in cosmic radiation are believed to be produced by the interactions of cosmic ray nuclei with interstellar space (ISM). Their production spectrum can be calculated and the propagation parameters obtained from the observed e^+ spectrum. Directly accelerated electrons dominate the e^- component. It is found that a simple power law injection spectrum for e^- can not explain the observed $[\mathrm{e}^+/(\mathrm{e}^+ + \mathrm{e}^-)]$ ratio, and one requires a spectral flattening below about 5 GeV. Flat e^- spectrum similar to that in Crab supernova with a spectral break by one power around 4.5 GeV could explain both the observed spectrum and the $[\mathrm{e}^+/(\mathrm{e}^+ + \mathrm{e}^-)]$, suggesting that the sources of cosmic ray e^- are Plerions in the Galaxy. The non-thermal spectrum from the Crab nebula is examined to show that cosmic ray electrons escape into the ISM only after about 2×10^4 yr. from the Plerions.

1 Introduction

Cosmic ray electrons being light leptons, suffer severe energy loss, by which their energy spectrum is considerably modified during propagation in the Galaxy. As a result, they provide the valuable tool to understand the propagation of cosmic rays and the physical state of the space where cosmic rays spent most of their time. The major energy loss processes they undergo are different from those of the nucleonic components. Below 1 GeV, Bremsstrahlung process is important and the radiation arising from this process contributes to a large fraction of the non-thermal background radiation in the γ-ray regime. At higher energies, the dominant energy loss mechanisms are the synchrotron radiation and inverse-Compton scattering, while traversing ambient magnetic and radiation fields respectively. While the energy loss due to these processes is proportional to the square of the electron energy, the former one leads to the emission of non-thermal radio background in the Galaxy over a broad band of frequencies and the latter one elevates the energy of ambient photons to X and γ-ray energies. Thus, the knowledge of the electron component plays an important role in the understanding of the propagation of cosmic rays, as well as on the origin of non-thermal radiation and the physical state of the region where this radiation comes from.

The electron component consists of both positive and negative particles. e^+ component is the end product of the decay of unstable particles, like pions and kaons, which are produced by the interaction of cosmic ray nucleons with the interstellar gas during their propagation. Estimates of the production spectrum of e^+ in the Galaxy were made in the past (eg: Daniel & Stephens, 1975; Protheroe, 1982; Moskalenko & Strong, 1998) and recently by Stephens (2001). They showed that the observed e^+ spectrum could be well understood as secondary particles. Knowing the production spectrum of e^+, one could then derive the propagation and solar modulation parameters from the measured e^+ spectrum. Unlike e^+, the observed $[\mathrm{e}^+/(\mathrm{e}^+ + \mathrm{e}^-)]$ clearly show that the cosmic ray e^- should have a large primary component. It was earlier found that the injection spectrum of this primary component is not a simple power law like that of nucleonic component (Stephens, 1999); it is flatter at low energies and steeper at high energies (Stephens, 2001). It is essential to know the sources which produce them. In this investigation, this aspect is examined by using different types of input spectrum for the primary e^-. From a comparison with the observations on e^- and $[\mathrm{e}^+/(\mathrm{e}^+ + \mathrm{e}^-)]$, it is shown that Plerions are main sources of cosmic ray e^- and they provide the necessary spectral break required in the electron injection spectrum. The observed spectrum of Crab nebula is then examined to determine the time scale required for the energetic e^- to escape into the ISM from the Plerions.

2 Propagation of electrons

Leaky-box model had been used for the propagation of the electron component, and the equation describing the propa-

Correspondence to: alfred@icepp.s.u-tokyo.ac.jp

gation can be written as (Stephens, 1990)

$$\frac{\partial N(E,t)}{\partial t} = \frac{\partial}{\partial E}\left\{N(E,t)\frac{dE}{dt}\right\} - \int_0^1 N(E)\psi_{rad}(v)dv + \int_0^1 N(\frac{E}{1-v},t)\psi_{rad}(v)dv - \frac{N(E,t)}{T^{es}(E)} + Q(E,t) \quad (1)$$

The first term on the RHS is the energy loss term, consisting of ionization, synchrotron and inverse-Compton scattering. The first integral term is for the Bremsstrahlung loss, which is not a continuous energy loss and the second is the gain of electrons from high energies due to Bremsstrahlung process. For considering ionization and Bremsstrahlung processes, the composition of ISM was assumed to consist of 80% neutral hydrogen, 10% ionized hydrogen and 10% helium nuclei. Further, proper energy derivatives of the continuous energy loss term had been carefully incorporated for the different expressions corresponding to the different composition. The next term is due to particle escape from the confinement region and the escape time T^{es} has a constant value of $T_0^{es} = 30$ Myr below 2.7 GV and is $T_0^{es}(2.7/E)^{0.5}$ above 2.7 GV, as determined from the abundance of radio clock nuclei (Streitmatter and Stephens, 2001) and B/C ratio (Stephens and Streitmatter, 2001).

In the case of inverse-Compton scattering, the energy loss in the two regions, Thompson limit and the Klein-Nishina limit, are given here (Blumental and Gould, 1970).

$$\frac{dE}{dt} = 1.0184 \times 10^{-16} E^2 \rho[1.0 - 0.03425E < \epsilon >] GeV/s \quad for \quad E \leq 14.599/ < \epsilon > \quad (2a)$$

$$= 3.605 \times 10^{-12} \frac{\rho}{< \epsilon >^2}[ln(E < \epsilon >) - 7.1525] GeV/s \quad for \quad E \geq 3193.3/ < \epsilon > \quad (2b)$$

Here, $< \epsilon >$ and ρ are the mean energy and the energy density of the photons in eV and eV/cc respectively. One can notice from the above equations, that in the Thompson limit, the energy loss is proportional to E^2 well below $14.6/ < \epsilon >$ GeV and there is a large gap between these two regions. In the case of scattering with star light photons, the E^2 dependence is valid only below about a GeV. The empirical fit that connects these two regions is (Stephens, 2001),

$$\frac{dE}{dt} = 6.313 \times 10^{-16} \frac{\rho}{< \epsilon >^2}[E < \epsilon >]^{1.061} \quad GeV/s \quad for \quad 14.599/ < \epsilon > \leq E \leq 3193.3/ < \epsilon > \quad (2c)$$

This expression provides the missing link between these two extreme regions, and the derivatives at the change-over energies show good continuity.

The steady state solution to the Eq.(1) was obtained by the method of Runge- Kutta technique until $\partial N(E)/\partial t \rightarrow 0$. Under the steady state condition, the production term in the Eq.(1) is independent of t. For this calculation, the interstellar density of hydrogen was taken to be 0.2 atom/cc corresponding to $T^{es} = 30$ Myr (Streitmatter and Stephens, 2001), as obtained from the study of radio-clock isotopes. The e^+ spectrum show that the observed data is consistent with $< \mathrm{B}_\perp >$ = 3 μ G and a star light density of 0.3 eV/cc (Stephens, 2001). These effective values include the variation over the regions in the halo, where cosmic rays are confined. It may be pointed out that at large energies, where lifetime due to energy loss is very small, one needs to consider the effect of nearby sources, and this requires the solution of diffusion equation both in space and time.

3 Electron spectrum

The production spectrum Q(E) for electron has two components, one is the secondary electrons arising from the interaction of cosmic ray nucleons with interstellar gas and the other from primary cosmic ray sources. The first component is taken from an earlier work (Stephens, 2001) by which the observed e^+ spectrum was well reproduced with the interstellar parameter discussed above and with a modulation parameter ϕ = 0.55 GV. For the second component, three kinds of spectra are considered in this investigation. They are discussed below.

3.1 Single power law injection spectrum

The observed nucleon spectra can be reproduced by an injection spectrum which is a power law in rigidity down to at least 100 MV. Therefore, it was assumed that the injection spectrum of e^- is a simple power law in energy $\mathrm{N(E)} = 210\mathrm{E}^{-2.5}\ \mathrm{e}^-\ /\ (\mathrm{m}^2.\mathrm{sr.s.GeV})$ (the production spectrum multiplied by the product of $\mathrm{T}_0^{\mathrm{es}}$, 4π and c). This spectrum was then added to the secondary spectrum of e^- and Eq. (1) was solved to obtain the equilibrium spectrum in the Galaxy. The equilibrium spectrum was then modulated using spherically symmetric solution with an equivalent modulation parameter ϕ = 0.55 GV as in the case of e^+ . The resultant spectrum is shown By curves denoted as B in Fig. 1 along with the measured flux values, which are multiplied by E^3. Though the data potted are from the published data over last 10 years, they too have a large scatter, especially in the region from about a GeV to a few tens of GeV, and not enough data exits above 100 GeV. The equilibrium spectrum in the Galaxy is shown by the dotted curve, while the dot-dashed curve is at the Earth. It can be noticed that in order to fit the data, one requires a larger modulation for e^- compared to e^+ .

The measured $[\mathrm{e}^+/(\mathrm{e}^+ + \mathrm{e}^-)]$ is shown as a function of energy in Fig.2. There still exits certain uncertainty in the measurements in the energy region from about 5 to 10 GeV and not much statistically significant data exist beyond 20 GeV. The dotted curve shown here as Curve B is the ratio in the ISM resulting from the single power law injection spectrum for e^- and the secondary e^+ spectrum. The dash-dotted Curve B is after modulating the ISM spectra of both e^- and

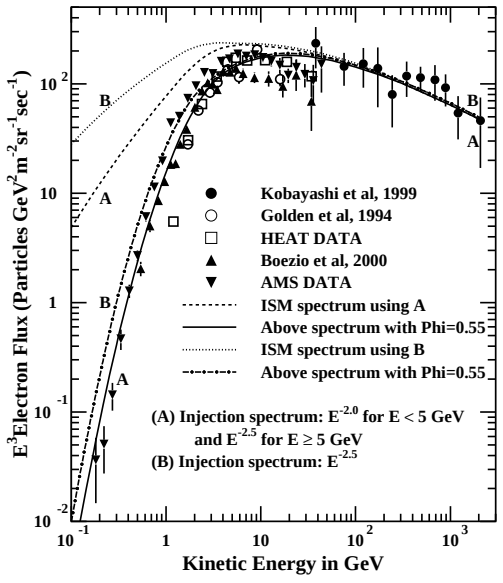

Fig. 1. The measured flux values are plotted as a function of energy and compared with calculated spectra with different injection spectra. The flux scale is multiplies by E^3.

e^+. The calculated ratios do not fit the data below 3 GeV. It is clear from this figure that single power law injection spectrum for cosmic ray primary e^- can not reproduce the observed $[\mathrm{e}^+/(\mathrm{e}^+ + \mathrm{e}^-)]$ and hence such a spectrum can be ruled out.

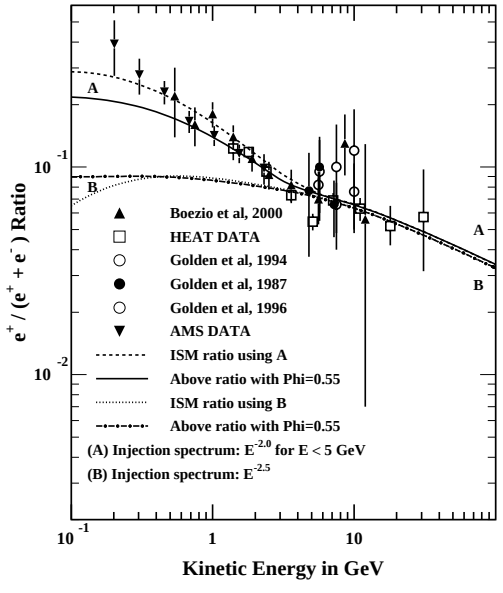

Fig. 2. The measured fraction of positrons is plotted as a function of energy and compared with expected fraction using different injection spectra for e^-.

3.2 Power law spectrum with a spectral break

Having failed to reproduce the observation using a single power law for the injection spectrum of primary e^-, both the spectrum of e^- and the e^+ fraction, it is necessary to examine a power law spectrum with a spectral break at a suitable energy. The justification for this also comes from the fact that the observed non-thermal radio spectrum in the Galaxy requires an electron spectrum in the ISM to be much flatter below about a few GeV (eg: Daniel and Stephens, 1975; Rockstroh and Webber, 1978). Therefore, an equivalent injection spectrum of the type, $90\mathrm{E}^{-2.0}$ e^- / $(\mathrm{m}^2.\mathrm{sr.s.GeV})$ has been considered with a spectral break $\Delta\beta$ = 0.5 at 5 GeV, which steepens the spectrum above this energy to β = -2.5. This spectrum is slightly different from that used earlier because of the inclusion of AMS data (Alcaraz et al., 2000).

The dashed curve marked as A in Fig.1 is the equilibrium spectrum of e^- in the ISM using the above injection spectrum and the solid curve is the spectrum at Earth using the same modulation parameter, which was derived from the e^+ spectrum. This modulated spectrum fits the data well compared that using a simple power law injection spectrum denoted by the Curve B. The expected $[\mathrm{e}^+/(\mathrm{e}^+ + \mathrm{e}^-)]$ as a function of energy, using the injection spectrum with a spectral break, is shown in Fig.2 by curves denoted as A. In this figure, the dashed curve is the ratio in the ISM and the solid curve is at the Earth. One can notice that these two curves differ below about 7 GeV due to the effect of solar modulation. It is also clear from this figure that though the expected ratio agrees with the measurement in a remarkable manner above a GeV, the observed ratio is much higher larger than the calculated curve as the energy decreases.

3.3 Plerion type spectrum

While the fit to the data is reasonably good using a power law spectrum with a spectral break, it is difficult to envisage a physical mechanism by which a spectral break of $\Delta\beta$ = 0.5 could be achieved from a source. The energy loss due to inverse Compton scattering and synchrotron radiation can make a spectral break by one power and the resultant equilibrium spectrum in a source can serve as the injection spectrum. Plerions as the source of e^- has been considered here, which have flat non-thermal spectrum. In the case of Crab nebula the measured spectral index is -0.27 from 0.01 to about 10^4 GHz. This corresponds to β = -1.54 for the radiating electrons. Therefore an injection spectrum of the type equivalent to $50\mathrm{E}^{-1.54}$ e^- / $(\mathrm{m}^2.\mathrm{sr.s.GeV})$ was considered with a $\Delta\beta$ = 1.0 at 4.5 GeV.

The equilibrium spectrum of e^- in the Galaxy using Plerion type injection spectrum is shown by the dashed curve in Fig. 3 and the modulated spectrum is shown by the solid curve. It can be seen from this figure that the fit to the data is better than that for a power law spectrum with a spectral break considered earlier. The resultant $[\mathrm{e}^+/(\mathrm{e}^+ + \mathrm{e}^-)]$ in the ISM and at Earth are shown in Fig. 4 by the dashed and dotted curves respectively. One can see the excellent fit to the

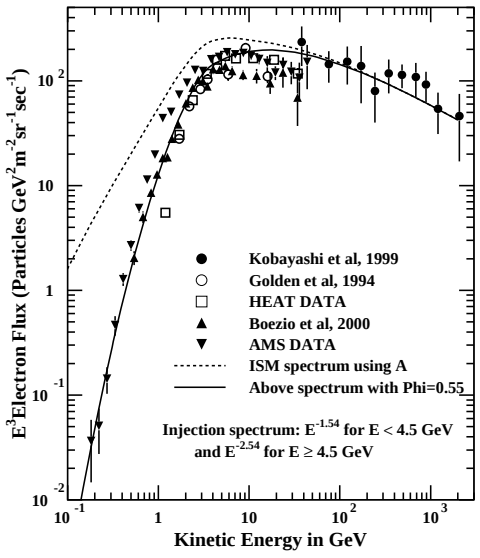

Fig. 3. The measured energy spectrum of electrons as in Fig. 1 is compared with calculated spectrum using an Plerion type injection spectrum

data at all energies. These good fits for both the spectrum and for the ratio clearly point to the important deduction that primary cosmic ray electrons are produced by the Plerions.

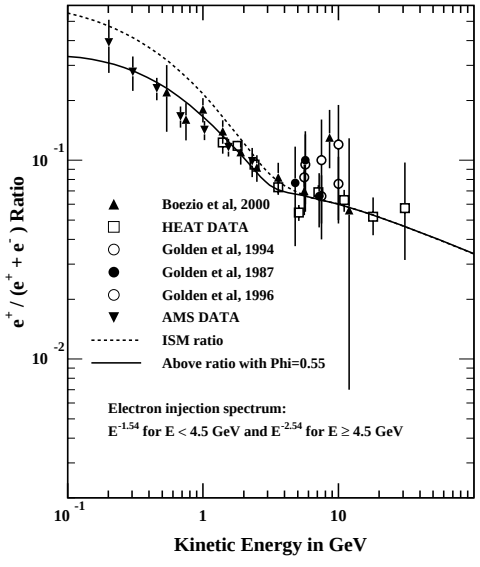

Fig. 4. The measured fraction of positrons is compared with the calculated ratio for the Plerion type injection spectrum for electrons

4 Crab nebula

From the above analysis, it is shown that the injection spectral shape of primary e^- is different from that of nucleons and it is probably produced by the Plerions. It is necessary to examine the physical state of the typical Plerion. Crab is chosen for this purpose as plenty of information is available. The non-thermal spectrum of Crab breaks by $\Delta\alpha \approx 0.5$ at about 1.4×10^4 GHz. Based on the assumption that the energy loss of e^- is dominated by synchrotron loss, Bietenholz et al.(1997) have shown that the break frequency corresponds to a field strength of $< \mathrm{B} >= 420\mu\mathrm{G}$. For a simple power law injection spectrum with only synchrotron radiation loss, one can show from Eq.(1) that the life time τ corresponds to an e^- break energy $\mathrm{E_B}$ = 4.5 GeV is $\tau_{\mathrm{Crab}} = 4.9\times10^5/[\mathrm{E_B} < \mathrm{B}_\perp >^2 (\beta-1)] = 2.6\times10^4\mathrm{yr}$. This would mean that the break frequency in the Crab will be lowered as it ages and $\mathrm{E_B}$ of 4.5 GeV required for the cosmic ray e^- will be attained after about 2×10^4 yr.

The observation also show that the spectral shape of the radiation does not show a change at least up to 5 GHz up to the edge of the nebula (Bietenholz et al., 1997). This may suggest that the radiating e^- are continuously produced and are confined to the nebula. At present Crab does not contribute to the galactic cosmic rays. It is possible that e^- will leak in to the ISM from Crab when the remnant disintegrates after τ_{Crab}. This may coincide with the time when $\mathrm{E_B}$ becomes close to 5 GeV. It is essential then to examine the characteristics of all known Plerions.

References

Alcaraz, J., et al., Phys. Lett., B 484, 10, 2000.
Barwick,S.W., et al., ApJ, **498**, 779, 1998.
Bietenholz,M.F., et al., ApJ, **490**, 291, 1997.
Blumenthal,G.R., and R.J. Gould, Rev. Mod. Phys., **42**, 237, 1970.
Boezio,M., et al., ApJ, **532**, 653, 2000.
Daniel,R.R., and S.A. Stephens, Sp. Sci. Rev., **17**, 45, 1975.
Golden,R.L., et al., ApJ, **287**, 622, 1984.
Golden,R.L., et al., A&A, **188**, 145, 1987.
Golden,R.L., et al., ApJ, **436**, 769, 1994.
Golden,R.L., et al., ApJ, **457**, L103, 1996.
Kobayashi, T., et al., Proc. 26th Int. Cosmic ray Conf. (Salt Lake City), **3**, 61, 1999.
Moskalenko,I.V, and A.W. Strong, ApJ, **493**, 694, 1998.
Muller,D., in 'Origin and Acceleration of Cosmic Rays', Ed. M. Israel, in Adv. sp. Res., 2001 (in print).
Rockstroh,J.M., and W.R. Webber, ApJ, **224**, 677, 1978.
Stephens,S.A., Proc. 21st Int. Cosmic Ray Conf. (Adelaide), **11**, 99, 1990.
Stephens, S.A., in 'Origin and Acceleration of Cosmic Rays', Ed. M. Israel, Adv. sp. Res., 2001 (in print).
Stephens,S.A., Astropart. Phys., **6**, 229, 1997.
Stephens,S.A., Proc. 26th Int. Cosmic Ray Conf. (Salt Lake City), **4**, 241, 1999.
Stephens,S.A., and R.E. Streitmatter, ApJ, **505**, 266, 1998.
Stephens,S.A., and R.E. Streitmatter, in 'Origin and Acceleration of Cosmic Rays', Ed. M. Israel, in Adv. sp. Res., 2001 (in print).
Streitmatter,R.E., and S.A. Stephens, Proc. 26th Int. Cosmic Ray Conf. (Salt Lake City), **4**, 199, 1999.
Streitmatter,R.E., and S.A. Stephens, in 'Origin and Acceleration of Cosmic Rays', Ed. M. Israel, Adv. sp. Res., 2001 (in print).